Model Estimation and Identification of Manual Controller Objectives in Complex Tracking Tasks

by

David K. Schmidt* and Pin-Jar Yuan**

School of Aeronautics and Astronautics

Purdue University

West Lafayette, IN

A methodology is presented for estimating the parameters in an optimal-control-structured model of the manual controller from experimental data on complex, multi-input/multi-output tracking tasks. Special attention is devoted to estimating the appropriate objective function for the task, as this is considered key in understanding the objectives and "strategy" of the manual controller. The technique is applied to data from single-input/single-output as well as multi-input/multi-output experiments, and results discussed.

---

*Professor

**Doctoral Candidate

Introduction

In this paper, we will present and apply a methodology for identifying from experimental data the parameters in a multi-input/multi-output model of manual control, suitable for analysis of complex tasks. In this context, "complex tasks" refers to tasks in which multiple loop closures are expected to be present, such as multi-axis tracking or aircraft landing approach, as opposed to compensatory tracking in the laboratory, for example. The structure of the model is compatible with the well-known[1] optimal-control model (OCM) of the human operator, and among the model-related parameters we seek to obtain is an estimate of the manual controller's objective function "weightings". This is considered important because by doing so, the modeler may obtain insight into the operator's strategy and perception of the task. Furthermore, the magnitude this function takes on has been hypothesized[2,3] to correlate with the operator's subjective rating of this task. Hence, an experimentally determined metric related to the subjective assessment of the task may hopefully result.

In addition to establishing a model structure useful for identification, we will also evaluate two procedures for the determination of the desired model parameters. One uses frequency-domain measurements, and as a result is similar to previous methods.[4,5] However, a variation on this technique will be presented to facilitate multi-input/multi-output model determination. The second procedure proposed is based entirely on time-domain data. As a result, the constraints on the experimental procedure, such as special tracking signals, required in the frequency-domain approaches are avoided. Results from both methods will be presented.

Model Structure

Since the model structure to be used is to be compatible with the OCM, we will briefly note its key features. Readers unfamiliar with this modeling approach are referred to the references. The hypothesis upon which the model is based is that the well trained, well motivated human controller chooses his control inputs (e.g. stick force) to meet his (internal) objective in the task, subject to his human limitations. This objective is further assumed to be expressible in terms of a quadratic "cost" function

$$J_p = E\left\{\lim_{T\to\infty}\frac{1}{T}\int_0^T (Y_p^T Q Y_p + u_p^T F u_p + \dot{u}_p^T R \dot{u}_p)dt\right\}$$

where Y_p = vector of human's observed variables (e.g., attitude, acceleration)

u_p = vector of his control inputs

Q,F,R = Controller-Selected (internal) weightings

The human limitations modeled include information-acquisition and processing time delay, observation and control input errors, and neuromuscular dynamics. A block diagram of the resulting model structure is shown in Figure 1.

The components of this model may be grouped into two parts, one dealing with the information acquisition and state estimation, and one related to the control law or control policy operating on the estimated state. As has been shown in the references on this modeling approach, the "solution" for the human's control inputs, as predicted by the model, is expressed as

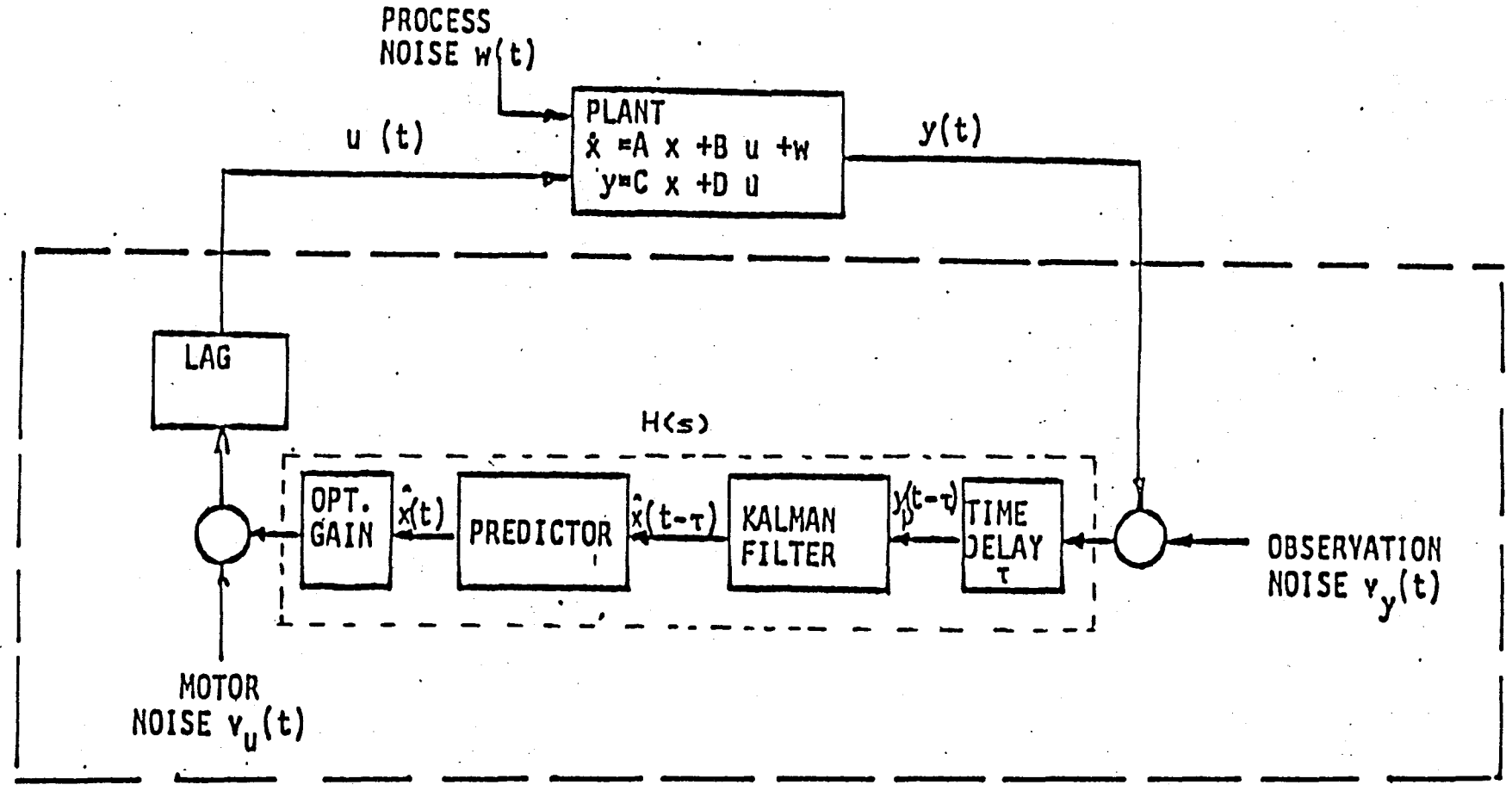

Figure 1. Optimal Control Model

$$\dot{u}_p = -G_x\hat{x} - G_u u_p + v_u \qquad (1)$$

where $\hat{x}$ = internal estimate of the system states

G_x, G_u = control gain matrices

v_u = motor noise, or control input errors

The system dynamics are taken as

$$\dot{x} = Ax + Bu_p \quad ; \quad y = Cx$$

where y = vector of system response

and if a tracking task is considered, the dynamics of the tracking signal vector y_c may be represented as

$$\dot{y}_c = A_c y_c + Dw$$

where w is a disturbance input of "white" noise. Usually, the tracking dynamics are combined with the system dynamics, resulting in an augmented state vector col[x,y_c]. Finally, the manual controller is considered to observe delayed system responses and commands, with some observation error, or

$$y_p = \begin{bmatrix} C_p x(t-\tau) \\ \hline y_c(t-\tau) \end{bmatrix} + v_y$$

where v_y = vector of observation errors. Usually, tracking error $\varepsilon = y_c - y$ is observed, plus the commands themselves if the task is that of pursuit. Additionally, other system responses may be observed but not actually regulated or tracked. Therefore, for our purposes we will arrange the human's observation vector as follows (dropping the $t-\tau$ here for brevity)

$$y_p^T = [\varepsilon^T, \dot{\varepsilon}^T, y_c^T, \dot{y}_c^T, y_o^T] + v_y^T$$

with $y_o = C_o x$ representing observed responses other than errors and commands. Clearly, the above expression can always be represented in the form

$$y_p = \bar{C}\bar{x}(t - \tau) + v_y$$

where $\bar{x}^T = [y_c^T, x]$ and $\bar{C}$ is partitioned accordingly to yield

$$\bar{C} = \begin{bmatrix} C_\varepsilon \\ \hline C_c \\ \hline C_o \end{bmatrix} \tag{2}$$

Reference 1, for example gives closed-form expressions for the state covariance matrix $E\{\chi\chi^T\}$ for this structure, under assumptions of independence and "whiteness" on w, v_u, and v_y. A compatible frequency domain representation of the manual controller may also be obtained that effectively has the following form

$$U_p(s) = T_n^{-1}(s)H(s)[Y_p(s) + N_y] + T_n^{-1}(s)N_u \tag{3}$$

where $Y_p(s)$ = Laplace Transform of $y_p(t)$ (not delayed)

$T_n^{-1}(s)$ = Neuromotor Dynamics (= $[G_n^{-1}s + I]^{-1}$ if Eqn. 1 is considered)

$H(s)$ = Manual Controller Transfer Function Matrix (Refer to Fig. 1)

N_y, N_u = Noise Vectors - Related to v_y and v_u

Also, the command and system dynamics expressed as

$$Y_c(s) = [sI - A_c]^{-1}DW(s) = \Phi_c(s)DW(s)$$

and

$$X(s) = [sI - A]^{-1}BU_p(s) = \Phi(s)BU_p(s)$$

may be combined to form

$$\chi(s) = \begin{bmatrix} Y_c(s) \\ X(s) \end{bmatrix} = \begin{bmatrix} \Phi_c(s)DW(s) \\ \Phi(s)BU_p(s) \end{bmatrix}$$

Then

$$Y_p(s) = \bar{C}\chi(s) = \begin{bmatrix} C_\varepsilon \\ \hdashline C_c \\ \hdashline C_o \end{bmatrix} \chi(s) \tag{4}$$

where recall $\bar{C}$ is partitioned as in Equation 2. If we now partition $H(s)$ and N_y to be compatible with $Y_p(s)$, we may let

$$H(s) \overset{\Delta}{=} [H_\varepsilon(s), H_c(s), H_o(s)]$$

$$N_y^T = [N_\varepsilon^T, N_c^T, N_o^T]$$

With this structure, we may represent the system as in Fig. 2, where we have used the following definitions

$$C_c \Rightarrow [I \vdots 0] \qquad (I = \text{Identity})$$

$$C_\varepsilon \Rightarrow [I \vdots -C_r]$$

and

$$C_o \Rightarrow [0 \vdots C_o]$$

to make the matrices have compatible dimensions. Note that not only is this structure consistent with the OCM with multiple inputs and outputs, but in the scalar case with $H_c = H_o = 0$ the structure also reduces to the conventional compensatory tracking block diagram. Shown in Fig. 3 is this simpler case.

For experimentally estimating a scalar $Y_p(j\omega)$, measurements are taken of $\Theta_c(t)$, $\varepsilon(t)$, and $u_p(t)$. Spectral analysis is then performed to obtain

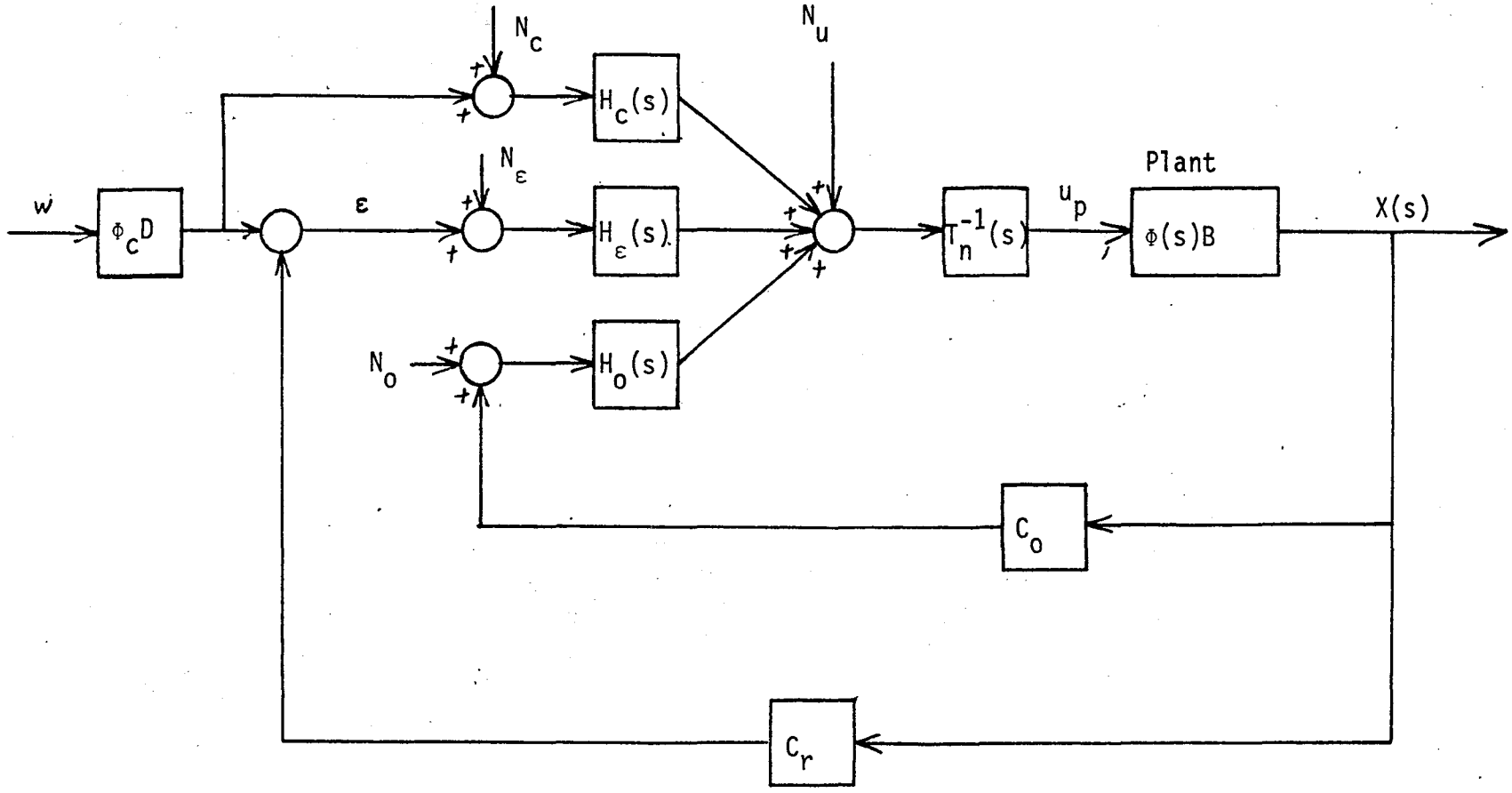

Figure 2. General Model Structure

$\Phi_{cu}(j\omega)$ = Cross spectrum between Θ_c and u_p

$\Phi_{c\varepsilon}(j\omega)$ = Cross spectrum between Θ_c and ε

and the desired relation is

$$Y_p(j\omega) = \Phi_{cu}(j\omega)/\Phi_{c\varepsilon}(j\omega)$$

which can be derived from block diagrm algebra (see for example Refs. 4 and 5).

Now, as discussed in Ref. 5, special experimental conditions must be invoked to identify multiple human operator transfer functions, as in H(s) discussed above. Specifically, independent excitation of all inputs to H(s) must be present, and this is frequently not possible in many practical situations. However, some alternate expressions will be developed which yield identifiable transfer functions directly related to the general model structure discussed here, but are not <u>human operator</u> transfer functions, like $Y_p(j\omega)$ in the scalar case cited above.

Referring to Eqns. 3 and 4 above, or equivalently Fig. 2, we have

$$U_p(s) = T_N^{-1}(s)[H_\varepsilon(s)(\varepsilon(s) + N_\varepsilon) + H_c(s)(Y_c(s) + N_c) + H_o(s)(Y_o(s) + N_o) + N_u]$$

$$\varepsilon(s) = Y_c(s) - C_r\Phi(s)BU_p(s)$$

$$Y_o(s) = C_o\Phi(s)BU_p(s)$$

Substituting $\varepsilon(s)$ and $Y_o(s)$ into the first expression, and solving for $U_p(s)$ yields

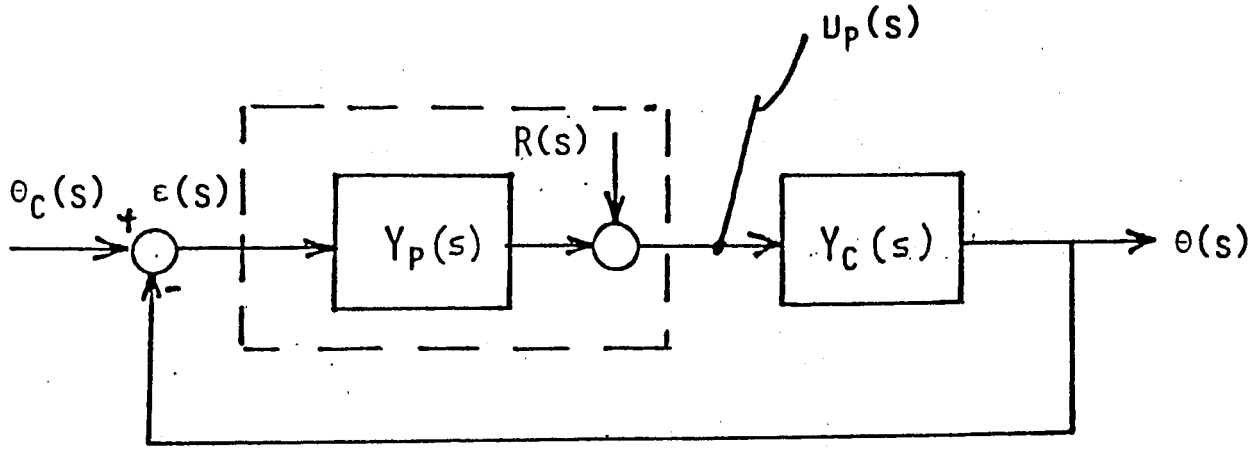

Figure 3. Scalar Model

$$U_p(s) = [T_{uc}(s)]Y_c(s) + [T_{uy}(s)]N_y + [T_{uu}(s)]N_u \tag{5}$$

where $N_y^T = [N_\varepsilon^T, N_c^T, N_o]$

$$T_{uc}(s) = [I + T_n^{-1}(s)\{H_\varepsilon(s)C_r - H_o(s)C_o\}\Phi(s)B]^{-1}[T_n^{-1}(s)\{H_\varepsilon(s)+H_c(s)\}]$$

$$T_{uy}(s) = [I + T_n^{-1}(s)\{H_\varepsilon(s)C_r - H_o(s)C_o\}\Phi(s)B]^{-1}[T_n^{-1}(s)[H_\varepsilon(s)\vdots H_c(s)\vdots H_o(s)]]$$

$$T_{uu}(s) = [I + T_n^{-1}(s)\{H_\varepsilon(s)C_r - H_o(s)C_o\}\Phi(s)B]^{-1}T_n^{-1}(s)$$

Substitution back into the relation for $\varepsilon(s)$ and $Y_o(s)$ yields

$$\begin{aligned} \varepsilon(s) &= [T_{\varepsilon c}(s)]Y_c(s) + [T_{\varepsilon y}(s)]N_y + [T_{\varepsilon u}(s)]N_u \\ Y_o(s) &= [T_{oc}(s)]Y_c(s) + [T_{oy}(s)]N_y + [T_{ou}(s)]N_u \end{aligned} \tag{6}$$

where

$$T_{\varepsilon c}(s) = [I - C_r\Phi(s)BT_{uc}(s)]$$

$$T_{\varepsilon y}(s) = -C_r\Phi(s)BT_{uy}(s)$$

$$T_{\varepsilon u}(s) = -C_r\Phi(s)BT_{uu}(s)$$

$$T_{oc}(s) = C_o\Phi(s)BT_{uc}(s)$$

$$T_{oy}(s) = C_o\Phi(s)BT_{uo}(s)$$

and

$$T_{ou}(s) = C_o\Phi(s)BT_{uu}(s)$$

Now the three transfer function matrices T_{uc}, $T_{\varepsilon c}$, and T_{oc} are related to the matrices of cross-spectra between u_p and y_c, ε and y_c, and y_o and y_c, respectively, assuming the "noises" N_y and N_u are uncorrelated with y_c. Or using matrix notation

$$\begin{aligned} T_{uc}(j\omega) &= [\Phi_{y_c u_p}(j\omega)][\Phi_{y_c y_c}(\omega)]^{-1} \\ T_{\varepsilon c}(j\omega) &= [\Phi_{y_c \varepsilon}(j\omega)][\Phi_{y_c y_c}(\omega)]^{-1} \\ T_{oc}(j\omega) &= [\Phi_{y_c y_o}(j\omega)][\Phi_{y_c y_c}(\omega)]^{-1} \end{aligned} \tag{7}$$

So, if frequency-domain data were used to estimate the above spectra, the transfer functions in Eqn. 7 may be identified, but not necessarily the elements of H(s). However, these identifiable transfer functions, due to their direct relationship to the OCM, for example, may be used for model identification and/or validation in exactly the same manner estimates for H(s) may be used, so they are just as meaningful.

Additionally, referring back to Equation 5, under the assumption that the noise vectors N_y and N_u consist of elements mutually uncorrelated, and uncorrelated with y_c, a model-related expression for the power of the remnant in each of the i'th components of u_p is expressible as

$$\begin{aligned} \Phi^i_{rr}(\omega) = &\sum_j |T_{u_i y_j}(j\omega)|^2 \Phi_{y_j y_j}(\omega) \\ &+ \sum_k |T_{u_i u_k}(j\omega)|^2 \Phi_{u_k u_k}(\omega) \end{aligned} \tag{8}$$

where $\Phi_{y_j y_j}(\omega)$ = Power spectrum of the j'th element in the noise N_y

$\Phi_{u_k u_k}(\omega)$ = Power spectrum of the K'th element in the noise N_u.

So if $\Phi^i_{rr}(\omega)$ is estimated experimentally, it is relatable to the model-based parameters on the right hand side of the above equation for further model comparison or validation. Similar expressions for all the above development are available in Ref. 6, for further reference.

Parameter Search Technique

Now that the model structure is obtained to allow direct comparisons between measured variables and their model-based counterparts, attention is now turned to obtaining the parameter set of interest. This parameter set, denoted p, consists of the "independent" variables of the model, such as objective function weights Q and R, time delay τ, and noise covariance matrices C_{n_y} and C_{n_u}, for example. We will make direct application of the quasi-Newton search approach of Refs. 5, 7 and 8, with two variations fundamental to our purpose. The first is that in the above references, a scalar objective function weight on tracking error alone was used exclusively, while we desire to estimate more complex expressions for the cost, or weighting matrices. Secondly, we will compare using two forms of experimental data, one strictly time domain and the other frequency domain, to determine if using only time domain data leads to sufficiently accurate results. This is desirable since a purely time domain approach is simpler and greatly reduces the requirement on the experimental technique for obtaining the required data.

The scheme is implemented to minimize a scalar matching cost of the form

$$M = \sum_{i=1}^{N} w_i e_i^2$$

where e_i is the difference between the i^{th} measured data point and the corresponding model prediction, w_i is a weighting coefficient. Or in matrix form:

$$M = e^T W e$$

with $e = \text{col}[e_1 e_2, \ldots]$, $W = \text{diag}[w_1]$.

For a trial set of model parameters p_1, we have its corresponding modeling cost

$$M_1 = e_1^T W e_1$$

For a new set of parameters $p_2 = p_1 + \Delta p$, we obtain a new modeling error Δe, related to Δp by

$$\Delta e = Q \Delta p$$

where $q(i, j) = \frac{\partial e_i}{\partial p_j}$ can be obtained by a numerical perturbation of the model. The change in the parameter vector Δp yielding the minimum modeling error, given the initial vector e_1 and the assumption of linearity between ΔM and Δp is

$$\Delta p = -[Q^T W Q]^{-1} Q^T W e_1$$

Thus an iteration procedure is established, which proceeds until no more improvement in matching cost M, or the required changes in the parameters in Δp are very small.

In addition to obtaining the best match to a given set of data, we also wish to determine some measure of the reliability of the identified

parameter values. A qualitative indication of parameter estimation reliability can often be obtained through sensitivity analysis relating changes in the scalar matching cost to perturbations in the model parameters. In general, estimates of parameters that have a high impact on the matching cost can be considered more reliable than estimates of parameters having a smaller impact.

As shown in Ref. 8, this sensitivity may be estimated from the relation

$$\Delta M_i = V^T Q^T W Q V (\Delta p_i)^2$$

where V is a column vector that has a value of unity for the i^{th} element and values for remaining elements V_r as determined from

$$V_r = -[Q_r^T W Q_r]^{-1} Q_r^T W q_i$$

where $q_i = \text{col}[q_{i,1}, q_{i,2}, \ldots]$ and the subscript r indicates vectors and matrices which omission of the ith row and column.

Pursuit Tracking Analysis

For comparing the time-vs. frequency-domain data for model determination, and to relate the above methodology to an established situation, a single axis pursuit tracking task is considered.[6] Subjects tracked a command signal generated by a sum of sinusoids

$$\Theta_c = \sum_{i=1}^{10} A_i \sin(\omega_i t + \phi_i)$$

for 100 seconds, with the frequencies ω_i evenly spaced between 0.25-17 rad/sec, and amplitudes A_i selected such that the spectrum of the command approximated a random signal generated by

$$\Theta_c/w = \frac{1}{s^2 + 3s + 2.25}$$

with "white" noise w intensity taken to be $\sigma_w^2 = 13.5\ \delta(t)$, - $\delta(t)$ a delta function.

In addition to Θ_c, the subjects observed the plant response $\Theta(t)$, and therefore the error $\Theta_c - \Theta$, where the two plants (Θ/δ_p) were K/s and K/s^2. A representative block diagram is shown in Figure 4. (Note the correspondence between this block diagram and that of Figure 2.) Since error, Θ_c, and Θ are not all linearly independent, only two need be included for observation. Therefore, the subjects observation vector may be taken as

$$y_p^T = [\varepsilon,\ \dot{\varepsilon},\ \Theta_c,\ \dot{\Theta}_c]$$

for both K/s and K/s^2 plants. Finally, including the subjects' control input δ_p in the state vector x, we may define

For K/s , $\quad x^T = [\Theta_c,\ \dot{\Theta}_c,\ \Theta,\ \delta_p]$

For K/s^2 , $\quad x^T = [\Theta_c,\ \dot{\Theta}_c,\ \Theta,\ \dot{\Theta},\ \delta_p]$

Referring back to Eqns. 5 and 6, one may consider $T_{uc}(s)$ and $T_{\varepsilon c}(s)$ to be scalars,

$$T_{uc}(s) = \frac{1}{\tau_n s+1}\,[H_1 + sH_2 + H_3 + sH_4][1 + F(H_1+sH_2)/(\tau_n s+1)]^{-1}$$

$$T_{\varepsilon c}(s) = [1 - F(H_3+sH_4)/(\tau_n s+1)][1 + F(H_1+sH_2)/(\tau_n s+1)]^{-1}$$

From the experimental data, the state covariance matrices $E[xx^T]$ were estimated, as well as the cross-spectra between Θ_c and δ_p, and Θ_c and ε (error), or $\Phi_{\Theta_c\delta_p}(j\omega)$ and $\Phi_{\Theta_c\varepsilon}(j\omega)$. Finally, although not possible in more complex situations, since $T_{uc}(s)$ and $T_{\varepsilon c}(s)$ are scalars in this case, an effective operator transfer function may be defined as

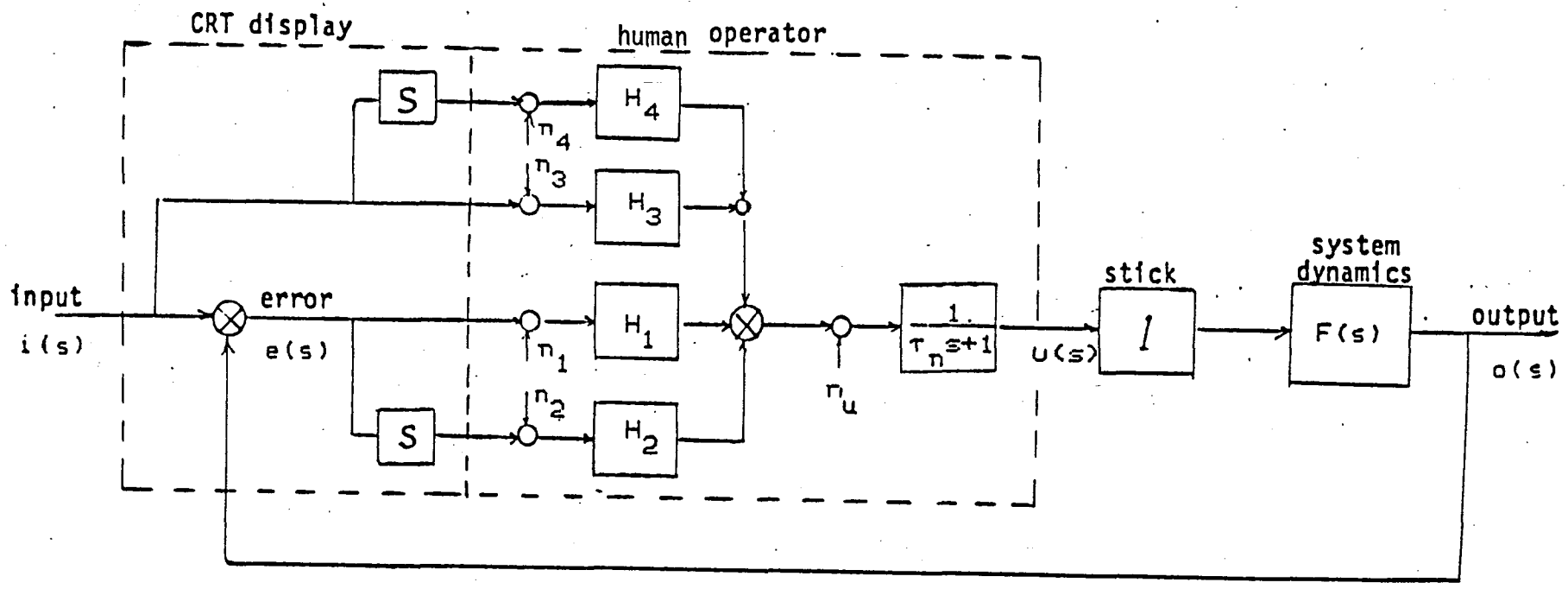

Figure 4. Pursuit Tracking Model Structure

$$y_{p_{eff}}(j\omega) \triangleq T_{uc}(j\omega)/T_{\varepsilon c}(j\omega)$$

$$= \Phi_{\Theta_c \delta_p}(j\omega)/\Phi_{\Theta_c \varepsilon}(j\omega)$$

These time and frequency-domain results were used for the quasi-Newton parameter search to estimate

$$p^T = [q_\varepsilon, q_{\dot{\varepsilon}}, \tau_n, \tau, C_{n_y}^T, C_{n_u}]$$

where q_ε, $q_{\dot{\varepsilon}}$ = objective function weights on error and error rate

τ_n = neuromotor time constant

τ = observation time delay

C_{n_y} = observation noise intensities (expressed as noise-to-signal ratios in dB relative to the variance of each observation)

C_{n_u} = motor noise intensity (expressed as noise-to-signal ratio in dB relative to control input variance)

Two separate parameter searches were performed. One used only the state covariance matrix for computing model matching cost, or

$$M_T = \frac{1}{N} \sum_{i,j}^{N} \left(\frac{X_{ij} - \hat{X}_{ij}}{\sigma_{ij}}\right)^2$$

where X_{ij} = element in experimentally-obtained state covariance matrix

$\hat{X}_{ij}$ = corresponding element from the covariance matrix from the model

σ_{ij} = standard deviation in the experimental value of X_{ij} over the repeated runs.

The second used only the frequency-domain result for $y_{p_{eff}}(j\omega_i)$,

$$M_F = \frac{1}{N}\sum_{i}^{N}\left[\left(\frac{G_i-\hat{G}_i}{\sigma_{G_i}}\right)^2 + \left(\frac{\psi_i-\hat{\psi}_i}{\sigma_{\psi_i}}\right)^2 + \left(\frac{R_i-\hat{R}_i}{\sigma_{R_i}}\right)^2\right]$$

where $G_i, \psi_i = |y_{p_{eff}}(j\omega_i)|$, and arg $y_{p_{eff}}(j\omega_i)$, ω_i input frequencies in command signal, measured experimentally from spectra

$\hat{G}_i$ $\hat{\psi}_i$ = corresponding magnitude and phase of the model-estimated transfer function

R_i = estimated power of the remnant in the control input δ_p, from experiment. Obtained from the spectrum of δ_p at frequencies other than those in the command.

$\hat{R}_i$ = remnant power obtained from the model (or Eqn. 8)

$\sigma_{G_i}, \sigma_{\psi_i}, \sigma_{R_i}$ = standard deviation of the experimental data

The estimates for desired model parameters p obtained using both approaches are listed in Tables 1 and 2, for the K/s and K/s^2 plants, respectively. Note the estimated values of the parameters do not differ significantly between the results obtained from minimizing M_T (time domain) and those from minimizing M_F (frequency domain). In some cases, the sensitivities in these costs to small relative changes in these parameters do vary, depending on whether frequency or time domain data is used.

Another interesting result is the comparison between the state covariance matrices obtained from the frequency-data - matched model and the time-data - matched model. The results for the K/s plant are given in Table 3, while those for K/s^2 are shown in Table 4. These results show not only excellent agreement with simulation results, but the result from the frequency-domain match agrees very well with the time domain

OCM pilot-related parameters	Time Match		Frequency Match	
	identification results	sensitivity	identification results	sensitivity
time delay, τ	.14 sec	.47	.13 sec	10.
weighting on error, q_ε	2707.	.19	2380.	.2
weighting on error, $q_{\dot{\varepsilon}}$ rate	348.	.09	377.	4.1
motor noise, c_{u_u}	-18. db	1.39	-18. db	3.2
observation noise of command, c_{y_c}	-6. db	.21	-7. db	2.2
observation noise of command rate, $c_{\dot{y}_c}$	-10. db	.68	-10. db	2.9
observation noise of error, c_ε	-11. db	.02	-11. db	3.5
observation noise of error rate, $c_{\dot{\varepsilon}}$	-10. db	.05	-10. db	3.4
neuromotor lag, τ_n	.09 sec			

Table 1. Matching Results - K/s Plant

OCM pilot-related parameters	Time Match identification results		Time Match sensitivity	Frequency Match identification result		Frequency Match sensitivity
time delay, τ	.10	sec	.65	.09	sec	10.
weighting on error, q_ε	2130.		.25	2320.		.1
weighting on error rate, $q_{\dot{\varepsilon}}$	319.		.18	380.		2.8
motor noise, c_{u_u}	-19.	db	1.20	-19.	db	.3
observation noise on command, c_{y_c}	-7.1	db	.48	-5.8	db	2.1
observation noise on command rate, $c_{\dot{y}_c}$	-7.5	db	.34	-9.5	db	1.4
observation noise on error, c_ε	-15.	db	.67	-11.	db	1.
observation noise on error rate, $c_{\dot{\varepsilon}}$	-9.7	db	.55	-10.	db	1.5
neuromotor lag τ_n	.20 sec					

Table 2. Matching Results - K/s^2 Plant

Table 3. Augmented State Covariance Matrix for K/s Plant

simulation result:

1.0	0.	.80	.46	θ_c(deg)
0.	2.25	-.46	.71	$\dot{\theta}_c$ (deg/sec)
.80	-.46	.93	-.1	θ (deg)
.46	.71	-.1	3.7	δ_p (in)

frequency domain match:

1.0	0.	.77	.28
0.	2.25	-.28	.91
.77	-.28	.76	0.
.28	.91	.0	3.5

time domain match:

1.0	0.	.79	.29
0.	2.25	-.29	.91
.79	-.29	.80	0.
.29	.91	.0	4.0

Table 4. Augmented State Covariance Matrix for K/s^2 Plant

simulation result:

1.0	0.	.73	.46	-.3	θ_c (deg)
0.	2.25	-.48	.13	1.8	$\dot{\theta}_c$ (deg/sec)
.73	-.48	1.27	0.	-3.	θ (deg)
.46	.13	0.	2.8	-.32	$\dot{\theta}$ (deg/sec)
-.3	1.8	-3.	-.32	35.	δ_p (in)

frequency domain match:

1.0	0.	.67	.39	-.36
0.	2.25	-.39	.36	2.0
.67	-.39	1.18	0.	-2.7
.39	.36	0.	2.7	0.
-.36	2.0	-2.7	0.	38.

time domain match:

1.0	0.	.73	.44	-.32
0.	2.25	-.44	.32	1.9
.73	-.44	1.24	0.	-3.0
.44	.32	0.	2.9	0.
-.32	1.9	-3.0	0.	41.

model, obtained by matching these statistics.

On the other hand, the frequency-matched model, as expected, matches that experimental data well, as shown in Figures 5 and 6. Note, furthermore, that the time-matched model does not do a poor job of matching this data as well.

From the above results, the following is noted:

1. The model obtained from time-domain matching is very close to the model obtained using frequency-domain data.
2. The sensitivity of the match to model parameter variations, however, differs between the time-and frequency-domain matches.
3. From the frequency-domain matches especially, the sensitivity of the match to variation in the cost function weighting on error rate, $q_{\dot{\varepsilon}}$, is quite large. This indicates that including this parameter in the cost function is significant.

Multi-Axis Tracking Analysis

As a final example, we will summarize the results of an analysis of a complex multi-axis tracking task.[9] The task involves fixed-base simulated air-to-air tracking, with the display symbology as shown in Fig. 7. The sight symbol (box) is dynamic, representing a lead-computing sight. It's position relative to the fixed screen reference is defined by the coordinates λ_{EL} and λ_{AZ}. The relative position of the target is defined by β_{EL} and β_{AZ}. And the relative bank angle ϕ_{Rel} between the target and attacker is indicated by the target's bank angle on the screen. (Note, ϕ_{rel} is zero for situation shown in the figure.) The linearized system dynamics are representative of tracking during a 4g, constant altitude turn. The input (or command) driving the closed-loop

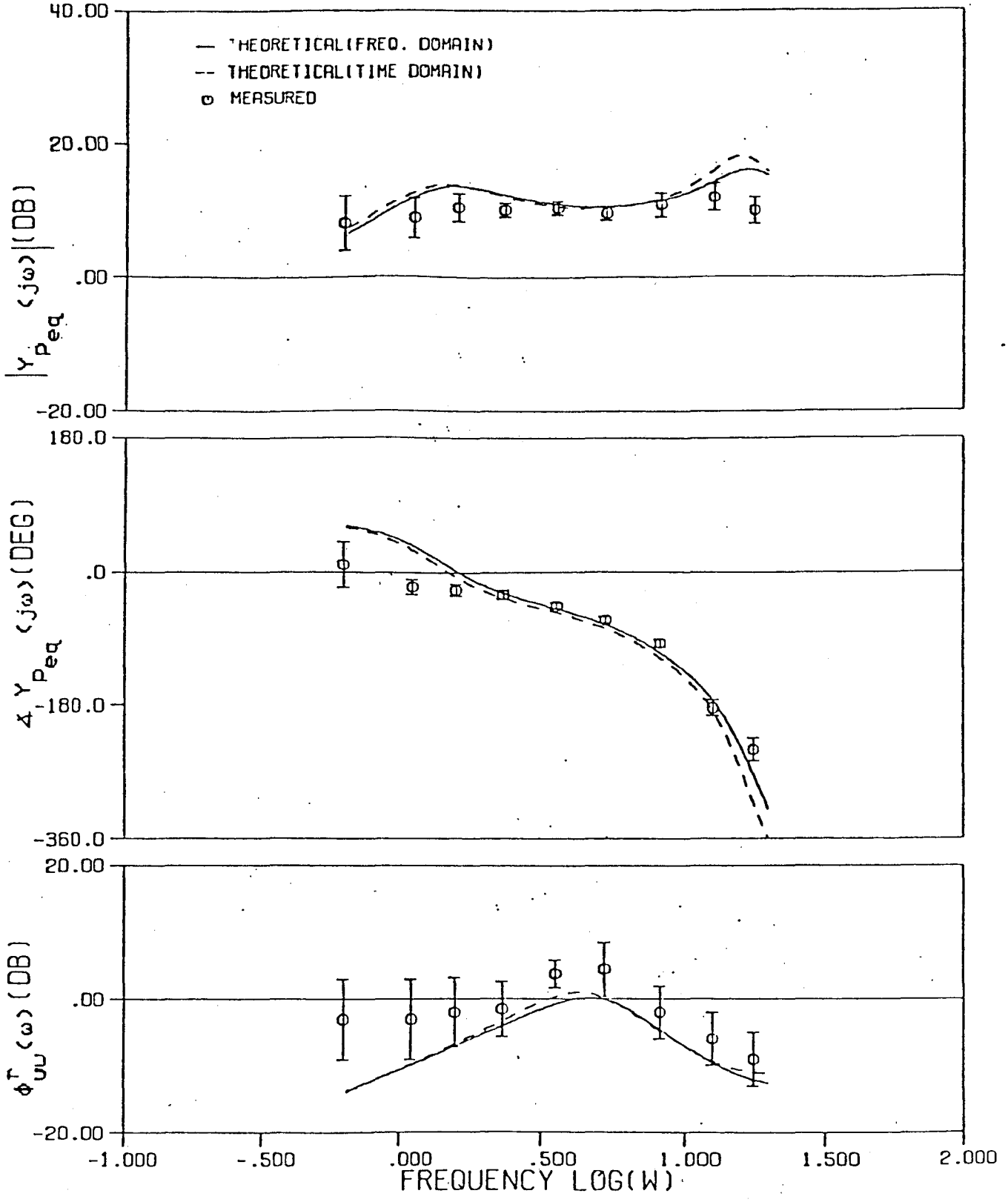

Figure 5. Human Describing Function and Controller Remnant-Correlated Spectrum of Simple Pursuit Task with k/s Plant

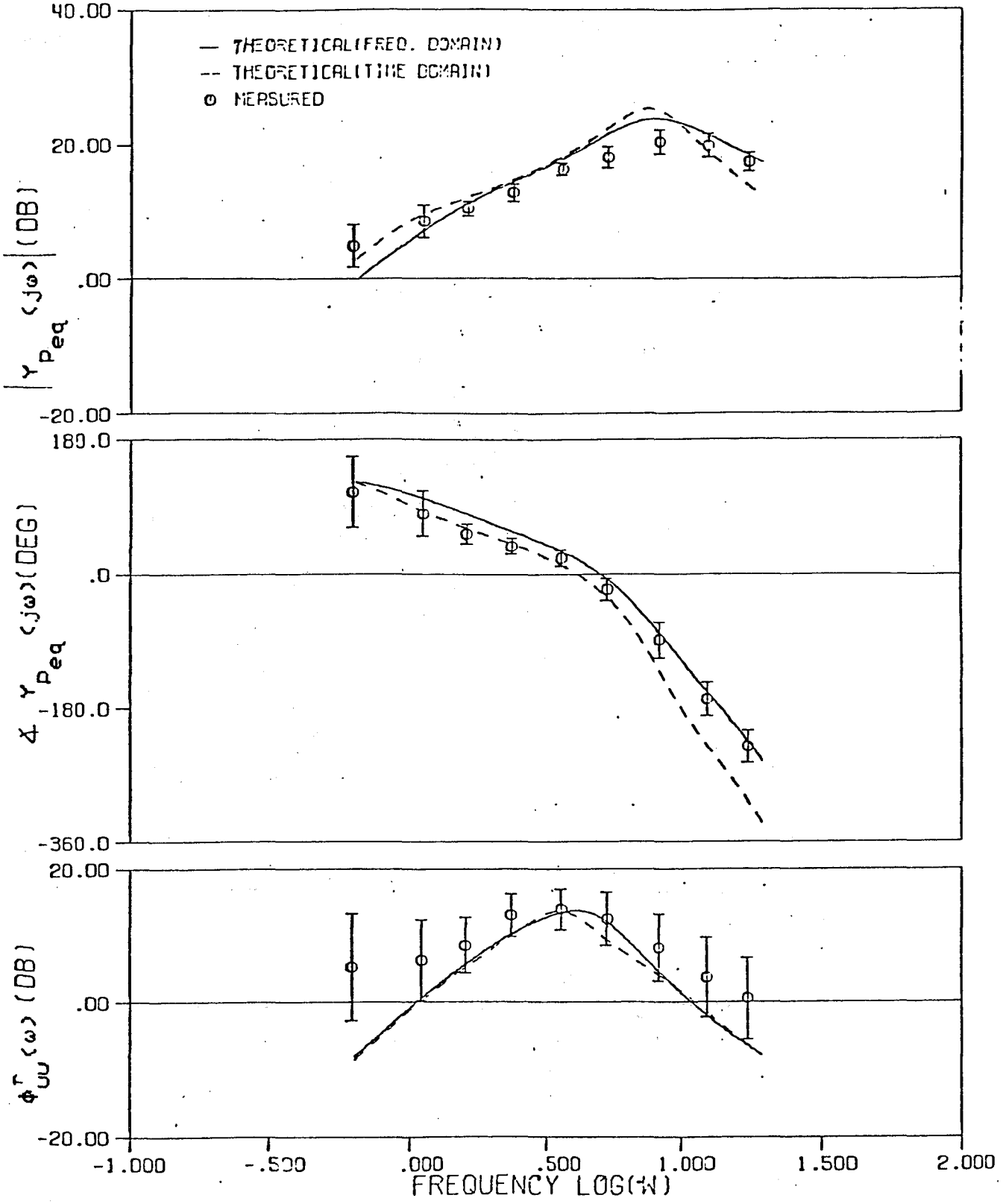

Fig. 6 Human Describing Function and Controller Remnant-Correlated Spectrum of Simple Pursuit Task with k/s^2 Plant

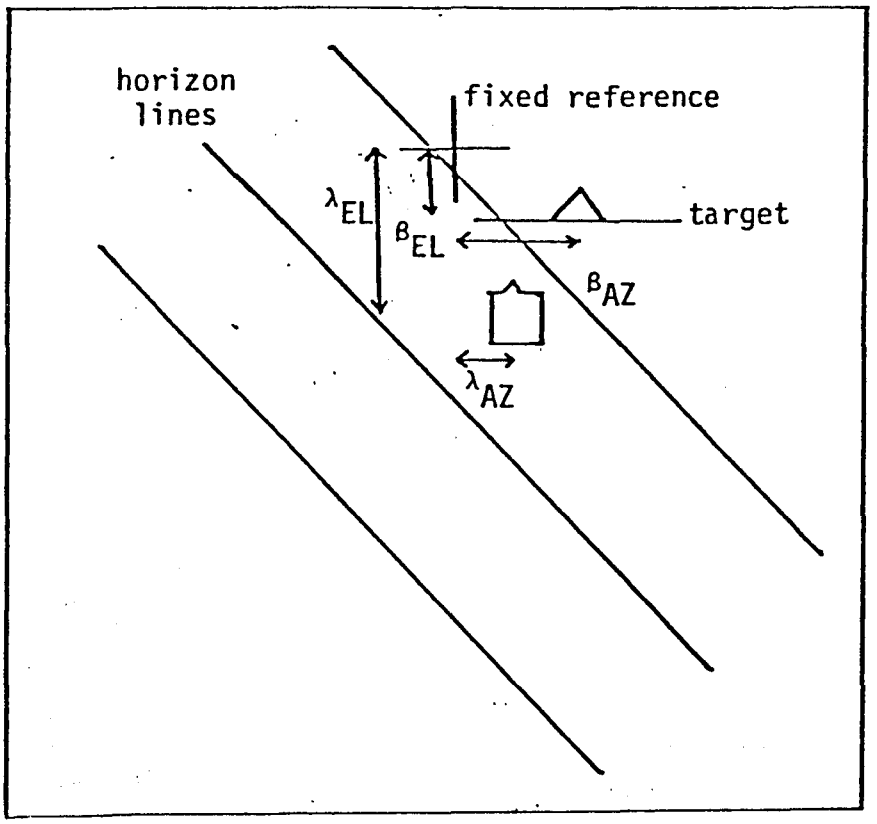

CRT Display for Multiaxis Air-to-Air Tracking Task

Fig. 7

system is the target's inertial (not relative) bank angle ϕ_T, which is generated by the relation

$$\dot{\phi}_T = -1/\tau\ \phi_T + w$$

with τ = 13 sec., and the intensity of the random w selected to yield an rms value of ϕ_T of 5.25 degrees.

One selected set of the pilot's observed variables is

$$y_p^T = [\varepsilon_{EL},\ \dot{\varepsilon}_{EL},\ \varepsilon_{AZ},\ \dot{\varepsilon}_{AZ},\ \beta_{EL},\ \dot{\beta}_{EL},\ \beta_{AZ}\ \ \dot{\beta}_{AZ},\ \phi]$$

where $\varepsilon_{(\cdot)} = \beta_{(\cdot)} - \lambda_{(\cdot)}$, tracking errors

ϕ = attacker's bank angle

Other combinations of observations could also be selected, and this set may not be optimum. Variations on this are under investigation. The pilot's control input is the stick and rudder, or δ_E, δ_A, and δ_R.

The model parameters will be estimated by a time-domain matching of the (16 x 16) state covariance matrix, including the three control inputs, obtained from several simulation runs. The parameter set to be discussed includes the (3 x 3) T_n matrix (or G_u^{-1}) associated with the three control inputs, the cost function weights

$$[q_{\varepsilon_{E1}},\ q_{\dot{\varepsilon}_{E1}},\ q_{\varepsilon_{AZ}},\ q_{\dot{\varepsilon}_{AZ}},\ q_{\beta_{E1}},\ q_{\dot{\beta}_{E1}},\ q_{\beta_{AZ}},\ q_{\dot{\beta}_{AZ}}]$$

and the noise intensities

$(c_{\delta_E},\ c_{\delta_A},\ c_{\delta_R})$ = Variances on motor noises

$(c_{\varepsilon_{E1}},\ c_{\dot{\varepsilon}_{E1}},\ c_{\varepsilon_{AZ}},\ c_{\dot{\varepsilon}_{AZ}})$ = Variances on measurement noises

The variances on the noises associated with the additional measurements

were fixed at - 13 dB after some initial studies.

As with the selected observation vector, the selection of cost function weights is based on subjective judgement, and one set may in fact be more meaningful than the other. For example, the use of a weighting on relative bank angle between target and attacker, rather than on β_{E1} and β_{AZ} could be considered. For the set selected here, however, the results are given in Table 5, and the T_n matrix is

$$T_n = \begin{bmatrix} .27 & 0 & 0 \\ 0 & .31 & -.15 \\ 0 & -.15 & .30 \end{bmatrix} \text{ (sec)}$$

for $$u_p^T = (\delta_E, \quad \delta_A, \quad \delta_R).$$

Note the relatively high sensitivity on the cost weightings on $\dot{\beta}_{EL}$ and $\dot{\beta}_{A2}$ in Table 5. This is consistent with the results of Harvey[10] in his evaluation of a similar single-axis task, in that weightings on observations in addition to tracking error and error rate were significant in obtaining a good model match. This fact is basic to the desire to be able to identify more complex cost functions, as noted in the introduction.

Finally, although this match used the simple-to-obtain state covariance matrix, comparisons or matching of frequency domain data is certainly possible if available from the experiment. If not, the frequency domain results from the model is available as a "prediction" of those human operator characteristics.

Note that slightly more general expressions for the transfer function matrices $T_{uc}(s)$, $T_{\varepsilon c}(s)$ and $T_{oc}(s)$ in Equations 5 and 6 result in the above example.[6] This arises due to the fact that the system dynamics

Table 5. Identification Result - Time Domain for Multiaxis Air-to-Air Tracking Task

OCM pilot-related parameters	identification results		sensitivity
time delay, τ	.13	sec	.2
weighting on elevation error, q_{E1}	1501.		3.4
weighting on eleva. error rate, $q_{\dot{E}1}$	340.		.1
weighting on azimuth error, q_A	1741.		2.4
weighting on azimu. error rate, $q_{\dot{A}}$	320.		.1
weight. on target elevation angle, $q_{\beta_{E1}}$	1575.		.2
weight. on target eleva. angle rate, $q_{\dot{\beta}_{E1}}$	248.		1.
weight. on target azimuth angle, q_{β_A}	1556.		.2
weight. on target azimu. angle rate, $q_{\dot{\beta}_A}$	226.		1.
elevator noise, c_{δ_E}	-21.3	db	2.0
aileron noise, c_{δ_A}	-20.6	db	.4
rudder noise, c_{δ_R}	-19.2	db	1.3
meas. noise on eleva. error, c_{ε_E}	-12.8	db	.8
meas. noise on eleva. error rate, $c_{\dot{\varepsilon}_E}$	-13.2	db	1.4
meas. noise on azimuth error, c_{ε_A}	-13.3	db	1.1
meas. noise on azimu. error rate, $c_{\dot{\varepsilon}_A}$	-13.2	db	.9

are not decoupled into command and plant dynamics, as assumed previously. As a result, the equation for $U_p(s)$ and $\epsilon(s)$ (Eqns. 5 and 6) are developed from the relation

$$\chi(s) = [sI - \bar{A}]^{-1}[\bar{B}U_p(s) + \bar{D}W(s)]$$

where

$$\bar{A} = \begin{bmatrix} A_c & A_c' \\ 0 & A \end{bmatrix}, \quad \bar{B} = \begin{bmatrix} 0 \\ B \end{bmatrix}, \quad \bar{D} = \begin{bmatrix} D \\ 0 \end{bmatrix}$$

In the development of Eqns. 5 and 6, A_c' in $\bar{A}$ was assumed zero. With this change, the development of the desired matrices proceeds directly, along with modifying Figure 2 accordingly.

Summary and Conclusions

An approach has been presented for identifying and/or validating multi-input/multi-output models for the manual controller in complex tracking tasks. In the more general case, the conventional human describing functions may not be directly identifiable, but measurable transfer matrices directly related to the model were derived. In terms of model identification or validation, these transfer matrices are just as useful and meaningful as the conventional describing functions.

Model-parameter identification using strictly time-domain data was demonstrated to yield excellent results for the single-axis pursuit task. The use of this approach avoids the necessity of obtaining frequency domain data, sometimes a practical constraint. However, shown in Ref. 11, time-series techniques may be used effectively to obtain frequency-domain representations directly compatible with the parameter identification method presented here. Furthermore, the time-series methods

would appear to circumvent several of the practical problems in obtaining frequency-domain representations - such as the necessity to be able to define the command signal characteristics. Therefore, model parameter estimation using frequency-domain representations are certainly of interest, and will remain useful.

The results obtained from evaluation of a two-axis air-to-air tracking task with complex, high-order dynamics were briefly noted, primarily to demonstrate the type of analysis possible with this approach.

Acknowledgement

This work is being performed with the cooperation of NASA Dryden Research Facility under NASA Grant NAG4-1. Mr. Donald T. Berry is the technical monitor, and his support, and that of NASA, is appreciated.

References

1. Kleinman, D., Baron, S., and Levison, W.H., "An Optimal Control Model of Human Response, Part I: Theory and Validation," Automatica, Vol. 6, 1970, pp. 357-369.

2. Hess, R.A., "Prediction of Pilot Opinion Rating Using an Optimal Pilot Model," Human Factors, Vol. 19, Oct. 1977, pp. 459-475.

3. Schmidt, D.K., "On the Use of the OCM's Objective Function as a Pilot Rating Metric," 17th Annual Conf. on Manual Control, UCLA, June, 1981.

4. McGruer, D.T., and Krendel, E.S., Mathematical Models of Human Pilot Behavior, AGARDograph, No. 188, Jan. 1974.

5. Levison, W.H., "Methods for Identifying Pilot Dynamics," Proceedings of the USAF/NASA Workshop on Flight Testing to Identify Pilot Workload and Pilot Dynamics, AFFTC-TR-82-5, Edwards AFB, Jan. 19-21, 1982.

6. Yuan, Pin-Jar, "Identification of Pilot Dynamics and Task Objectives From Man-in-the-Loop Simulation," Ph.D. Dissertation, School of Aeronautics and Astronautics, Purdue University, May, 1984.

7. Lancraft and Kleinman, "On the Identification of Parameters in the OCM," Proc. of the Fifteenth Annual Conf. on Manual Cont., Wright State Univ., Dayton, OH, Mar. 1979.

8. Levison, "A Quasi-Newton Procedure For Identifying Pilot-Related Parameters of the OCM," Proc. of the 17th Annual Conf. on Manual Control, UCLA, Los Angeles, June, 1981.

9. Yucuis, "Computer Simulation of a Multi-Axis Air-to-Air Tracking Task and the Optimal Control Pilot Model," M.S. Thesis, School of Aeronautics and Astronautics, Purdue University, Dec., 1982.

10. Harvey, T.R. "Application of an Optimal Control Pilot Model to Air-to-Air Combat," AFIT Thesis GA/MA/74M-1, Mar., 1974.

11. Biezad, D. and Schmidt, D.K., "Time Series Modeling of Human Operator Dynamics in Manual Control Tasks," Proc. of the 20th Annual Conf. on Manual Cont., NASA Ames Research Center, CA, June, 1984.